

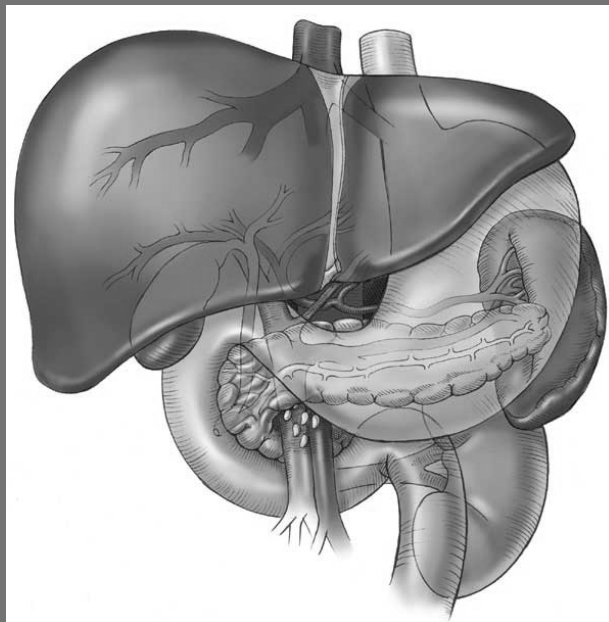
# Modelling of diaphragm motion for simulation of liver access

Surgery and Anaesthesia BSc Project

Supervisor: Dr. Fernando Bello

Co-supervisor: Dr. Pierre-Frédéric Villard

5351 Words



Metesh Nalin Acharya



## **Surgery and Anaesthesia BSc Project**

### **Modelling of Diaphragm Motion for Simulation of Liver Access**

**11 February – 16 May 2008**

Student: Metesh Nalin Acharya  
metesh.acharya@imperial.ac.uk

Supervisor: Dr. Fernando Bello  
Senior Lecturer in Surgical Graphics and Computing  
Division of Surgery, Oncology, Reproductive Biology and  
Anaesthetics  
f.bello@imperial.ac.uk

Co-supervisor: Dr. Pierre-Frédéric Villard  
Research Associate in Surgical Graphics and Computing  
Division of Surgery, Oncology, Reproductive Biology and  
Anaesthetics  
p.villard@imperial.ac.uk

Address: Department of Biosurgery and Surgical Technology  
Imperial College London  
10<sup>th</sup> Floor QEQM Building  
St. Mary's Hospital  
Praed Street  
London  
W2 1NY

Word count	Abstract	298
	Introduction	2057
	Method	1748
	Results	708
	Discussion	540
	Total	5351

## **Abbreviations used within text**

<b>3D</b>	Three-dimensional
<b>4D</b>	Four-dimensional
<b>CT</b>	Computed Tomography
<b>DICOM</b>	Digital Imaging and Communications in Medicine
<b>HCC</b>	Hepatocellular Carcinoma
<b>KB</b>	Kilobytes
<b>MB</b>	Megabytes
<b>MIS</b>	Minimally Invasive Surgery
<b>MR</b>	Magnetic Resonance
<b>PEI</b>	Percutaneous Ethanol Injection
<b>RMS</b>	Root Mean Square
<b>RFA</b>	Radio-Frequency Ablation

## ABSTRACT

**Purpose** To generate a realistic three-dimensional model of human diaphragm motion, using CT and MR data, for incorporation into virtual reality simulators.

**Background** Liver surgery and radiotherapy, for which targeting positions is crucial, are often complicated by displacement secondary to breathing. This may hinder accurate instrument placement during minimally invasive surgery or compromise the therapeutic dose achieved in tumour tissue. Since the diaphragm is the major determinant of respiratory motion, it is important to study its activity during the respiratory cycle. Incorporation of diaphragm motion models into virtual reality simulators will enhance the accuracy of tumour targeting and liver access simulation, and aid surgical education.

**Methods and Materials** A literature review was performed to establish segmentation criteria for the diaphragm. 4D CT data, displaying ten breathing phases of the respiratory cycle, was sourced retrospectively from two different patients undergoing lung radiotherapy. Additional MR data, consisting of three breathing phases, was obtained from a healthy volunteer. The diaphragm was manually segmented and a 3D mesh generated, for two phases of the 4D CT data and for three phases of the MR data, using Insight SnAP™ software. Non-rigid registration of the initial to final breathing phases was performed using Insight Segmentation and Registration Toolkit™ (ITK) software. The geometric differences obtained from non-rigid registration were compared using MESH™ software. Finally, standard algorithms are applied to the segmented data sets to produce smooth 3D reconstructions of the diaphragms which were used in a virtual reality simulator.

**Results** We present a 3D model of diaphragm motion, which considers physiological boundary conditions, rib and sternum kinematics, and the muscular and tendinous aspects of the diaphragm.

**Conclusion** The validation results suggest that the diaphragm model proposed closely resembles the behaviour of the human diaphragm. It may be integrated into virtual reality simulators of liver access procedures or into radiotherapy treatment planning software.

**Keywords** Diaphragm; segmentation; breathing motion; diaphragm model; surgical simulation; liver surgery; virtual reality

## INTRODUCTION

In *Aphorisms*, Hippocrates, the father of medicine, alludes to the challenges of surgical education that we face today: “Life is short, the Art long, opportunity fleeting, experience deplorable and judgement difficult” (The Internet Classics Archive, 1994). Surgical training has traditionally embraced the apprenticeship model, whereby young trainees are entrusted to the care of a master surgeon (Cosman *et al*, 2002). Novice surgeons acquire skills in an opportunistic manner, initially observing experienced surgeons at work, before progressing onto performing the less troublesome operations under direction. This is the intrinsic flaw of the apprenticeship system – that despite extended training periods spanning many years, a young surgeon may fail to gain sufficient experience in the most challenging procedures, owing to selective and unequal exposure to the spectrum of surgical diseases (Dawson and Kaufman, 1998). With the operating theatre representing the most common, and perhaps the only legitimate setting for the realistic demonstration of surgical techniques (Basdogan *et al*, 2007), and with teaching costs estimated at \$25 per minute (Dawson and Kaufman, 1998), such practice is neither conducive to patient safety, nor cost-effectiveness. The previously adopted “see one, do one, teach one” philosophy is now facing harsh criticism.

The report *To Err is Human* (Institute of Medicine of the National Academy of Sciences, 2000) estimated that more people die each year in the United States from medical mistakes (44,000) than from motor vehicle accidents (43,458), breast cancer (42,297) or AIDS (16,516). This may be attributed to the relative inexperience of novice surgeons in

comparison with their superiors – who may also struggle as newer, safer, and more cost-effective techniques are gradually introduced into surgical contexts otherwise dominated by time-honoured, conventional practices (Basdogan *et al*, 2007). Advances in medical technology, whilst augmenting patient care, inadvertently generate training ‘voids’ that threaten the apprenticeship system. The recent expansion in minimally invasive surgery (MIS, or laparoscopy) practices, for instance, was facilitated by the availability of miniaturised video cameras capable of excellent image reproduction (Darzi and Mackay, 2002) the Hopkin rod lens, and powerful suction and insufflation devices (Jaffray, 2005). The apprenticeship system is failing to arm surgeons with the entirely different skill sets necessitated by such innovative techniques (Roberts *et al*, 2006).

MIS employs long, customised instruments that are introduced into the body via smaller incisions than those in open surgery. This affords reduced postoperative pain, a shorter hospital stay, quicker recovery of normal function, and perhaps most importantly for the vigilant patient, improved cosmesis (Aggarwal *et al*, 2004; Jaffray, 2005). However, certain procedures are hampered by longer operating times, associated with increased treatment expenses and usage of disposable supplies (Hart and Karthigasu, 2007; Jaffray, 2005). Potentially severe cardiopulmonary complications can occur, some of which are exclusive to the laparoscopic mode of entry (Sharma *et al*, 1997). The acquisition of proficiency in laparoscopy is a time-consuming process, as reflected in steep learning curves (Aggarwal *et al*, 2006); surgeons must first become accustomed to certain physical and visual constraints posed by MIS.

Highly developed psychomotor skills are required to manipulate cumbersome surgical tools within a three-dimensional operating environment that is portrayed on a monoscopic, two-dimensional video screen. This, coupled with a lack of co-axial illumination, jeopardises visual depth perception (Hanna *et al*, 2002; Mishra *et al*, 2004); a narrow field of view limits visualisation of internal organs (Basdogan *et al*, 2007). Long, thin, rigid instruments present ergonomic difficulties and diminish the haptic (tactile and force feedback) cues (Lee *et al*, 2007a; Lee *et al*, 2007b), which would otherwise assist the surgeon's interpretation of the operating site. Additionally, the rotation of instruments around the entry ports (fulcrum effect) makes direct translational movements impossible and disturbs the eye-hand-target axis (Basdogan *et al*, 2007; Roberts *et al*, 2006).

Aspiring laparoscopic surgeons should not be intimidated by these problems. After all, technical aptitude has repeatedly been cited as a characteristic of the successful surgeon (Cuschieri *et al*, 2001; Moorthy *et al*, 2003; Morton, 2000; Sarker and Patel, 2007). It is the daily performance of complex, procedural tasks utilising a great deal of manual dexterity that generally differentiates surgeons from their physician colleagues (Sarker and Patel, 2007). Other aspects of surgical competency – such as knowledge base, effective decision-making and team-working (Sarker and Patel, 2007) – are reviewed during the foundation years of surgical practice, yet technical skills assessment is often over-looked, despite being the major determinant of patient outcome (Fried *et al*, 2004). Indeed, the teaching and testing of technical skills has been reported as the least systematic or standardised component of surgical education

(Reznick, 1993). Some 23% of trainees lack formal assessment during one of their surgical placements, whilst a remarkable 70% do not even receive regular appraisal (Hart and Karthigasu, 2007). Furthermore, there is an increasing prevalence for the laparoscopic management of certain surgical diseases; laparoscopic cholecystectomy is now well established as the 'gold standard' therapy for 75% to 95% of gallstone cases (Visser *et al*, 2008) and many other procedures are currently being validated (Darzi and Mackay, 2002). This warrants the implementation of robust training strategies, as an adjunct to surgical curricula already in place at medical institutions, that are capable of sustaining a surgeon for the duration of his/her career.

There are many reasons for the apparent shortcomings in current surgical training programmes. Interventional radiology and procedural medicine have succeeded in cutting operating lists, forcing surgical trainees to acquire proficiency away from the operating room and in shorter time periods (Cosman *et al*, 2002; Moorthy *et al*, 2003). There is now compelling evidence advocating medical and/or conservative therapy in conjunction with, or replacement of, the surgical management of disease. In liver cancer, for example, only 5-10% of patients represent candidates for potentially curative surgical resection due to the presence of advanced disease. However, the correct delivery of radiotherapy can afford patients improved survival and often durable disease control (Al-Nahhas, 2007; Krishnan *et al*, 2008). The cost of training surgical residents in the operating theatre is becoming prohibitively expensive; one source estimates a figure of \$53 million for 1,014 general surgery residents that graduated in 1997 in the US (Bridges and Diamond, 1999). This coupled with intense medicolegal pressures to

boost hospital productivity, restricted working hours following the implementation of the European Working Time Directive (Pickersgill, 2001) and the ever-present fear of litigation (Hart and Karthigasu, 2007) has had far-reaching consequences for the surgical training system. These points demand an exploration into alternative avenues for the progression of surgical education.

Virtual reality simulation presents one possible solution to this dilemma. For over fifty years, the aviation sector has enjoyed the merits of simulation training, allowing the rehearsal and certification of pilots' flight skills, without posing any threat to passengers and squandering precious fuel commodities. The successful extrapolation of this concept for medical applications gave rise to the first, albeit primitive, surgical simulator (Satava, 1993).

In a surgical context, virtual reality is defined as “the use of a computer to generate an environment of surgical relevance based on specific mathematical models with which humans can interact using physical representations of surgical instruments” (Seymour and Røtnes, 2006). Developers must address five key areas for surgical simulators to achieve significant face validity - namely fidelity, object properties, interactivity, sensory input and reactivity (Satava, 1993). A realistic depiction of the underlying human anatomy and physiology are required. Tissues and organs must be rendered in sufficiently high-resolution, along with accurate texture and colour profiles. They must be susceptible to grasping, clamping and slicing (Satava, 1993; Satava 2001a) and

mimic the body's physiological responses to surgical manipulation, by bleeding or leaking fluid when cut, for example. Complex mathematical models are required to accommodate the geometric and topological changes in organ structure that subsequently occur (Seymour and Røtnes, 2006). The integration of haptic technology – the combination of tactile and kinaesthetic perception – enhances the overall experience greatly (Westebring-Van Der Putten *et al*, 2008).

Surgical simulators may assist skills acquisition, assessment and retraining. They provide the opportunity for the repeated practice of critical skills in a controlled, protected environment. Whereas patient-centred teaching is only possible at certain peak times, a freely accessible simulator would allow trainees to fit their self-directed learning around their work commitments (Cosman *et al*, 2002). Similarly, trainees can develop proficiency whilst working at their own pace (Dunkin *et al*, 2007), in an education-orientated environment free from the performance pressures of the operating room. Multiple trainees can attain a specified skill level on the same simulator, prior to honing their skills on real patients, thus achieving standardisation of training (Aggarwal *et al*, 2006). The simulation can be interrupted at will, allowing time for a supervisor to instruct the user through the more demanding parts of the procedure, and addressing any particular problems s/he may have (Aggarwal *et al*, 2006; Cosman *et al*, 2002). The entire simulated procedure can be recorded, stored digitally and played back, encouraging self-review and objective assessment (Sarker and Patel, 2007). Instant feedback, based on the quantitative performance measures, such as operational accuracy, hand motion economy and degree of unnecessary tissue damage, is obtained

at the end of a procedure (Basdogan *et al*, 2007; Moorthy *et al*, 2003). Most importantly, the surgeon is afforded the 'freedom to fail' without any adverse consequence (Satava, 2001b). Simulator training avoids the ethical, moral and cost implications of working on animal models (Roberts *et al*, 2006); certain patient-associated risks, such as infection transmission, are also eliminated. As Cosman *et al* (2002) elegantly put it, surgical simulators have "the potential to save patients from trainees, and trainees from patients".

The applications of surgical virtual reality have expanded to include liver and lung radiotherapy and image-guided liver access procedures. Hepatocellular carcinoma (HCC) is the most common liver cancer and ranked as the fifth most common type of cancer worldwide (Higgins and Berger, 2006; Lencioni *et al*, 2005). Image-guidance is needed for the precise targeting of suspicious intrahepatic masses to maximise diagnostic yield from biopsy (Clifford *et al*, 2002).

Whilst surgical resection is reserved for patients with asymptomatic HCC and well-preserved liver function (Llovet and Beaugrand, 2003), radiotherapy, radiofrequency ablation (RFA), cryotherapy and percutaneous ethanol injection (PEI) comprise the mainstay of treatment for the large majority (Dick *et al*, 2002; Gillams, 2005). RFA uses electrodes percutaneously directed onto the tumour, through which a high-frequency alternating current induces coagulative necrosis (Adam, 2002; Lencioni *et al*, 2004; Lencioni and Crocetti, 2005); intra-tumoural ethanol administration exerts direct

cytotoxic effects in PEI (Clark, 2007). Cryotherapy causes irreversible tumour tissue destruction at temperatures of less than  $-20^{\circ}\text{C}$  (Adam, 2002; Dick *et al*, 2002). The accurate identification and targeting of pathological tissue is paramount here to minimise undesirable complications arising from collateral damage to healthy tissue. RFA risks intraperitoneal bleeding, bile duct injury and hepatic abscess formation (Higgins and Berger, 2006), whilst haemorrhage, pleural effusion and tumour lysis syndrome are associated with cryotherapy (Hinshaw and Lee, 2007). Hepatic surgery simulators incorporating these interventional techniques may help to reduce the occurrence of such adverse events (Baegert *et al*, 2007; Marescaux *et al*, 1998; Müller *et al*, 2007; Reitinger *et al*, 2006; Villard *et al*, 2005).

The applications of external beam radiotherapy in liver cancer have been limited by the liver's notoriously poor radiation tolerance; if sustained over excessively long periods, even therapeutic doses may be harmful (Hawkins and Dawson, 2006; Krishnan *et al*, 2007). The safe administration of escalated radiation doses capable of tumour shrinkage have only recently been possible through advances in diagnostic imaging, three-dimensional planning, and image-guided radiotherapy (Hawkins and Dawson, 2006; Krishnan *et al*, 2007; Tse *et al*, 2008).

Breathing, as a source of liver interfractional motion, introduces error into laparoscopic liver access and the delivery of liver radiotherapy (Rietzel *et al*, 2005). Treatment margins must be widened to encompass estimated tumour trajectories in an attempt to

compensate for the unpredictability of tumour motion, further complicated by liver elasticity (Kirilova *et al*, 2008). Optimal radiation doses achieved in tumour tissue are compromised and healthy tissue is subjected to potentially lethal irradiation (Mutaf and Brinkmann, 2008).

The liver has been quoted as the “the most moveable (abdominal) organ in both respiration and standardised breathing” (Suramo *et al*, 1984). Liver displacement secondary to tidal breathing occurs primarily along the cranio-caudal axis, in the range of five to fifty millimetres (Balter *et al*, 2001; Davies *et al*, 1994; Suramo *et al*, 1984). This is largely determined by diaphragmatic activity: the liver’s falciform, left triangular and right coronary ligaments are attached to the diaphragm, subjecting it to considerable respiratory-related deformation.

The diaphragm is a fibromuscular sheet, separating the thoracic and abdominal cavities. Its peripheral muscle fibres form two hemispheric domes under each lung, before converging onto a central tendon (Drake *et al*, 2005; Gale, 1986). It is attached anteriorly to the xiphoid process of the sternum and to the lower six ribs and their costal cartilages comprising the costal margin (Drake *et al*, 2005). It passes posteriorly, under the heart and lungs, to attach to the anterolateral surfaces of the lumbar vertebrae (L 1-3 on right, L1-2 on left) via two musculotendinous pillars (crura) and to the ends of ribs eleven and twelve (Panicek *et al*, 1988). Whilst the anterior-posterior and transverse dimensions of the thorax are augmented by the ‘hinge’ movement of the sternum, and

the 'bucket handle' elevation of the ribs respectively, the diaphragm expands its vertical dimension by contracting downwards and drawing air into the lungs (Drake *et al*, 2005). In quiet respiration, only the domes descend; however, the central tendon is depressed from the T8 to T9 level in deep breathing, to accommodate larger lung volumes (Sinnatamby, 1999).

Intra-operative organ deformation secondary to breathing and surgical manipulation impedes instrument placement in minimally invasive and interventional radiology procedures, and is as yet an unresolved issue. Methods of minimising the unwanted effects of breathing motion, such as active breathing control (Dawson *et al*, 2001), forced breath-holding, respiratory gating (Giraud *et al*, 2006) and the use of external markers (Vedam *et al*, 2003) have been proposed; such techniques may be difficult to implement in elderly patients, who are frequently the recipients of interventional radiotherapy procedures.

It is therefore the aim of this study to generate a realistic three-dimensional model of the human diaphragm, constructed from CT and MR data, in order to characterise its motion. Secondly, we anticipate the incorporation of our diaphragm model into virtual reality simulators of liver access procedures utilising haptic technology, or radiotherapy treatment planning software. This will benefit surgical training by improving the realism and accuracy of hepatic surgery simulation and will also provide a better understanding of breathing motion as pertains to liver radiotherapy.

## **METHODS AND MATERIALS**

The study aim of generating a 3D model of the human diaphragm was split into eight smaller tasks: (i) a review of relevant literature and background reading, (ii) acquisition of patient data, (iii) manual image segmentation, (iv) registration-based segmentation, (v) quantitative validation, (vi) mesh generation and modelling and (vii) visual validation.

### **I. Literature Review and Background Reading**

Detailed anatomic knowledge and background reading on the current were required prior to commencing this study. An initial search in the PubMed database was conducted using various combinations of the search terms “diaphragm”, “anatomy”, “visualization”, “imaging”, “CT” and “MRI”. This however yielded only few useful papers. To supplement this, two widely-read anatomy textbooks (Drake *et al*, 2005; Sinnatamby, 1999) were consulted, which proved useful in the acquisition of fundamental anatomical knowledge. In particular, it was important to understand the physiological action of the diaphragm and to establish its boundaries, as dictated by its various attachments. A more specialised insight into human anatomy in the context of radiology was gained by studying relevant sections in a radiology textbook (Weir and Abrahams, 2003). Importantly, the principles of interpretation of radiologic images were easy to learn from the clear, well-annotated slides and would form the basis for later work involving CT and MR scans. During the course of the study, additional literature searches in PubMed database were performed, to facilitate the understanding of related topics as they emerged. Links between diaphragm motion and the fields of surgical education, virtual

reality simulation, liver cancer and its interventional management became clearer, and strengthened the study rationale. After carefully scrutinising the characteristics of similar published studies conducted previously, it was possible to modify our methodological approach accordingly, to avoid repetition of study design. This helped to increase the originality of our intended work, whilst fitting it into the broader context of the current knowledge base in the field.

## **II. Acquisition of Patient Data**

### ***Patients***

This study entailed the retrospective analysis of patient imaging and was approved following review by an ethical committee. Existing 4D thoracic CT datasets were retrospectively selected for two patients undergoing lung radiotherapy, one from each of two reputable cancer units - the Centre Léon Bérard in France and the Siemens Heidelberg therapy centre in Germany – that work in close collaboration with our academic institution, St. Mary's Hospital in London. The CT datasets were named 'CLB' and 'Siemens' accordingly, for ease of reference. A complementary 4D thoracic MR study of a volunteer from our department was performed at the Royal Liverpool University Hospital in England, and subsequently termed 'MRI'. The CLB and MRI datasets contained an information file providing variable additional information regarding the scans, but this was unavailable for the Siemens data. In any case, the anonymous nature of this file meant that it was not possible to trace the patients, and there was no indication of patient age, gender, height or weight.

MR offers superior soft tissue visualisation especially near bony structures and is thus particularly suited to study of the diaphragm. However, CT allows precise geometrical information regarding anatomical structures, in addition to physical tissue properties, to be obtained. For this reason, we chose to employ both CT and MR modalities.

### ***Scanning Protocols***

Helical CT scanning of the supine CLB patient was commenced on 8 February 2007 using a Philips Brilliance CT Big Bore scanner with oncology configuration. The scanning parameters were: 2 mm slice thickness, 2 mm slice spacing, 120 kVp, 120 mA, 0.4 second rotation time, 60 cm scanning field of view, voxel size 0.98 x 0.98 x 2.00 and a resolution of 1.024 pixels per mm; the acquisition time was six seconds.

Scanning for the supine MRI patient was carried out on a 1.5T Philips Achieva machine using a four-element SENSE body coil. The scanning protocol was: 3 mm slice thickness, 4 mm slice spacing, echo time 4.59 seconds, repetition time 102.5 ms, flip angle of 80°, 272 phase-encoding steps, acquisition matrix 272 x 272, phase field of view 79.4%, voxel size 0.71 x 0.71 x 4.00 and a resolution of 1.403 pixels per mm; the acquisition time was unknown.

The scanning protocols used for the Siemens patient are unspecified due to the retrospective selection of the imaging dataset.

### ***Acquired Imaging Data*** (Table 1, p31)

Respiratory synchronisation facilitates the identification of scanned images according to their position within the respiratory cycle. It provides a temporal correlation between any given scanned image and the corresponding position of the diaphragm at a particular phase in the breathing cycle. Each image is assigned a specific respiratory phase label. Now, an image dataset has been generated, comprising of spatio-temporally consistent volumes of data, with each volume containing axial, coronal and sagittal views of the thorax.

The 705 MB CLB dataset consisted of scanned images of the thorax at ten phases of the respiratory cycle. At each phase, the scanned image was saved as both an hdr file of approximately 70 MB, and also a much smaller 1 KB img file to facilitate computer retrieval.

The slightly larger 717 MB Siemens dataset contained ten folders for ten breathing phases. Each contained between 281 and 287 images, indicating the number of CT slices comprising the 'slab' of data. The Siemens dataset shared the popular DICOM file format with the MRI dataset. Only images representing a reference, intermediate and final breathing state were available in the MRI dataset.

As the CLB and Siemens datasets were compiled from previously completed imaging studies, they were uploaded to our institution's secure file transfer system, along with the MRI dataset. The images were now prepared for segmentation.

### III. Manual Image Segmentation (Figure 1, p33)

The segmentation of internal organs is an important, but difficult task in the quantitative analysis of medical images (Dhawan and Arata, 1993; Rangayyan *et al*, 2008; Kang *et al*, 2004). It is defined as “the division of a volume into multiple areas or objects with distinct features” (Qatarneh *et al*, 2003). Manual segmentation can be achieved through the complex, visual analysis of size, shape, location, texture, intensity and proximity to surrounding structures (Qatarneh *et al*, 2003), although several automatic techniques can attain excellent results.

ITK-SNAP is an operator-assisted tool developed for the segmentation of volumetric medical imaging; it is freely available from <http://www.itksnap.org/>. Its main window displays three orthogonal cross-sections of the loaded image, emphasising the often-ignored 3D nature of medical images (Yushkevich *et al*, 2006). A panel on the left encourages user interaction: a crosshairs tool allows a cursor to be strategically positioned at the same point in all three planes and a zoom function allows useful magnification of a single or multiple slices simultaneously.

The manual segmentation of the diaphragm is both time-consuming and arduous, and requires a trained expert. Starting inferiorly from where the diaphragm is most clearly delineated, the user makes a series of clicks around the target area and forms a closed contour using the polygon tool (Yushkevich *et al*, 2006). The contour framework can be edited by moving, inserting and deleting selected vertices. A colour label is then assigned to the outlined structure. This process must be repeated over many consecutive slices; the labels can then be exported as a 3D surface model.

#### **IV. Registration-Based Segmentation (Figure 2, p34)**

Registration is “the determination of a geometrical transformation, or mapping, from points in one image to points in another image” (Rohlfing *et al*, 2004; Zitová and Flusser, 2003). Image registration is classified as either rigid, where only translations or rotations are necessary to achieve correspondence between two structures in different images, or non-rigid, where local deformations must also be accounted for (Crum *et al*, 2004; Maintz and Viergever, 1998; Vidal *et al*, 2006). Non-rigid techniques are further classified as sparse vector field methods or dense vector field methods (Sarrut *et al*, 2005); we were interested in the latter. Diaphragm motion is a complex phenomenon, and non-rigid registration techniques must be applied to accommodate the local deformations between breathing phases in the respiratory cycle.

We sought to compute a geometric transformation that could be used to propagate a set of defined points from a reference diaphragm segmentation (at 0% inhalation), to a segmented diaphragm representing a final (100% inhalation) breathing state. Thus, a 4D model of diaphragm motion could be obtained.

The Image Registration Toolkit (ITK), freely available from <http://www.doc.ic.ac.uk/~dr/software/download.html>, was used to perform the non-rigid registration in a three stage process.

1. A target image filename is initially entered into a Windows© command line, followed by a source image filename - both must be in gipl format. A filename for the estimated transformation that maps points in the target file to matching points in the source file must also be specified with a .dof extension. An example of this first step is given:

```
C:\nreg [target.gipl] [source.gipl] -dofout [transformation.dof] (1)
```

2. A second command line is necessary to propagate the transformation obtained in (1) (named transformation.dof) from the source image file onto a 'predicted' diaphragm (named predicted.gipl) in a final breathing phase. The second command line, would thus read as follows:

```
C:\ttransformation [source.gipl] [predicted.gipl] -dofin [transformation].dof (2)
```

3. This process generates an image file of a predicted diaphragm, which must be opened within the ITK-SNAP segmentation tool. Finally, the 3D surface model of this predicted diaphragm is saved in .stl format, ready for quantitative validation.

Non-rigid registration was performed once for each of the CLB and Siemens datasets (0% inhalation and 90% inhalation; 0% exhalation and 100% inhalation, respectively). It was carried out twice for the MRI dataset, between phases 1 and 2, and 1 and 3.

## V. Quantitative Validation

The geometric differences between the 3D surface models of the predicted diaphragms (named registered models) and those from the source image files (named segmented models), can be compared. Both the segmented and registered 3D models are first converted into .ply format and subsequently opened in MESH software. The largest mismatch error between the contours of the 3D models is calculated as the Hausdorff distance (Huttenlocher *et al*, 1993). These errors are depicted using a colour spectrum applied to the model surfaces.

## VI. Mesh Generation and Modelling

Computer-based reconstruction of the 3D surface models entails the application of standard algorithms (Smith *et al*, 2004). A Gaussian filter smoothens gaps between slice contours. A triangular mesh is built onto the model surface by way of a Marching Cubes algorithm, to which a Laplacian smoothing process is finally applied.

Diaphragm motion modelling is coded using Java 3D API which affords real-time adjustment of simulation parameters, including rib kinematics and depth of breath (Villard *et al*, 2008). The tendinous aspect of the diaphragm is modelled with a tensegrity system; a mass-spring system is applied to the muscular component.

## **VII. Visual Validation**

This was an important step in ensuring the anatomical accuracy of our developing simulation. We regularly assessed the physiological behaviour of our model, discussing ways it could be improved, and validating it against existing, commercial models of respiratory motion. We were able to improve our diaphragm model significantly in these ways, by checking that diaphragmatic displacement was proportional to the muscular forces exerted and carefully considering rib and sternum motion, for example. In one of our preliminary motion models, the diaphragm was relaxing rapidly, yet contracting in an almost passive manner. Visual validation assisted our correction of this model.

## RESULTS

The primary aim of this study was to create an accurate three-dimensional model of the human diaphragm, which was segmented from CT and MR data. Non-rigid image registration was performed estimate diaphragm position at any time-point within the respiratory cycle. Quantitative and visual analysis was conducted for validation purposes. The results obtained in this study will now be presented.

### ***Segmentation Results*** (Figure 3, p35)

Our original plan was to segment the diaphragm in as many breathing phases per dataset as possible. However, it became readily apparent that such practice would be both impractical in face of time restrictions and would not provide additional benefit towards our study. An initial comparison between the segmented 0% and 90% inhalation phases of CLB dataset revealed only slight variations in the dimensions of the 3D surface models obtained, and these changes would be even harder to discern with segmentations of diaphragms from consecutive breathing phases.

Segmentation of each CLB and Siemens dataset took approximately twelve hours, whereas each MRI dataset took seven hours. In the initial phase of the MRI dataset only 34 slices in the axial plane required segmenting; the greatest number of slices that were segmented was 54, in the third phase. In contrast, the Siemens dataset comprised the greatest workload with more than 90 axial slices needing segmentation; only half this number was obtained with the CLB dataset.

A visual comparison of the best segmentations from each dataset is provided by figure 3. Whilst segmentation was a slow process initially, the segmentations produced are generally of sufficiently high quality for incorporation into diaphragm models.

### ***Results from Non-Rigid Registration (Figure 4 p36, Figure 5 p37, Table 2 p32)***

The registrations, especially of images from larger datasets, were very computer-intensive. CT-based registration took considerably longer than that for MR, at ten hours versus two hours.

The Hausdorff distance represents the maximum surface distance between the 3D surface models from registered and segmented images. The left-sided images in figure 4 depict the Hausdorff distance between the surfaces of the diaphragm extracted from CT scan at the initial and final breathing states within a dataset. The right-sided images in figure 4 represent this distance between the diaphragm surfaces at the simulated final and true final breathing states. For the Siemens dataset in figure 4A, there is a good correlation between the two diaphragm surfaces as indicated by the extensive blue colour of the diaphragm. In the case of the Siemens dataset, the mean absolute distance error is approximately 1.53 mm, although slightly more distance error is observed in the posterior regions of the diaphragm surfaces. Within the CLB dataset, although the mean absolute distance error is less than 0.5 mm greater than that of the Siemens dataset, these small distance errors occur over a larger area of the diaphragm, accounting for the green patches in figure 4. Taken together, these results suggest that CT is an excellent modality for diaphragm imaging.

The Hausdorff values obtained from the MRI datasets were dramatically different, and indicated large discrepancies between the 3D surface models from registered and segmented MR images. Absolute mean errors exceeding 30 mm occurred; the greatest errors, as highlighted by red and yellow in figure 5, occur over the diaphragm domes, perhaps because these areas are most affected by respiratory motion. Alternatively, the registration process may have been flawed and did not appropriately estimate the final breathing phase, or the segmentation of the initial breathing phase was of a poor quality. Whilst the average of the absolute mean distance errors of the Siemens and CLB CT datasets remains low at 1.35 mm, this same parameter reaches 21.86 mm when the MR modality is used. Interestingly, the maximum absolute error increases in a disproportionate manner from 35.9 mm to 87.7 mm as there is a larger diaphragm displacement between the MRI dataset's first and third breathing phases, than between the first two alone. Improvements in MR acquisition strategies will need to be implemented to improve diaphragm visualisation.

### ***Final Diaphragm Model (Figure 6, p38)***

Our proposed diaphragm model incorporates a manually segmented diaphragm from a real patient and a thoracic cage that was segmented automatically using simple threshold and morphological operations. Physiologically accurate diaphragm activity is modelled according to normal, tidal breathing; the ribs expand and contract in synchrony with the diaphragm to realistically simulate breathing.

## DISCUSSION

Our results show that whilst MR imaging may afford enhanced characterisation of soft tissue structures, and potentially the diaphragm, resolution and contrast may suffer. Nevertheless, with emerging applications of high-resolution MR, improved thoracic imaging will become possible. We were able to obtain several high quality diaphragm segmentations constructed from CT datasets. Both quantitative and qualitative studies have confirmed the validity of our CT-based results.

The modelling of diaphragm motion is an important task, and has been the topic of much research in the past. Behr *et al* (2006) successfully extracted diaphragm contours from post-mortem subjects and proposed a mathematical model of the diaphragm for use in virtual traumatology. Using dynamic echo-planar MR imaging, Craighero *et al* (2005) achieved three-dimensional reconstruction of the diaphragm during the respiratory cycle and also quantified the in-vivo properties of the diaphragm. Recent respiratory motion simulations have generated significant interest in diaphragm modelling (Didier *et al*, 2007). We have attempted to build on this existing knowledge by suggesting the incorporation of realistic diaphragm models into surgical simulators.

Surgical simulation is a rapidly developing field. With the advent of innovative new procedures necessitating advanced technical skills and decreased exposure to intra-operative surgical training, virtual reality simulation is being investigated as a means to teach and test these core abilities. Critically, simulation training must be incorporated as part of a fully endorsed surgical curriculum.

Our study has several limitations which could be addressed in future work. The CT and MR data obtained was of variable quality and image analysis was occasionally affected by poor resolution and the presence of artefacts. By optimising scanning protocols, superior imaging would be obtained; the resolution and contrast of the preliminary imaging data has a direct impact on the ease of segmentation. The large volumes of imaging data posed certain logistical challenges and required

Segmentation is itself a time-consuming and labour-intensive process, requiring a computer-literate user with a considerable background medical and anatomical knowledge, especially regarding radiological image analysis. Owing to time constraints, we had to limit the number of breathing phases in which the diaphragm was segmented. This did not seem to detract from the significance of our results, and could be explored in more detail in the future. Perhaps automatic segmentation strategies could be designed specifically for the diaphragm; however, experience with such techniques so far with diaphragm segmentation has been disappointing.

Some of the computer programmes used in this study required considerable processing power and were prone to crashing on older machines. The ITK registration toolkit in particular required several hours just to compute one image registration; furthermore, the use of command lines to operate this programme was unusual and confusing. A drawback of the registration-based segmentation processes adopted in this study is that the accuracy of registration is dependent on segmentation.

There is significant inter-patient variability in diaphragm structure (Gale, 1986). Thus the final model of diaphragm motion may not be applicable to all patients. Future work in

this field would involve the addition of patient-specific parameters, such as total lung capacity, and tidal volume.

## **CONCLUSIONS**

A three-dimensional, anatomically truthful diaphragm model is presented, taking into account relevant physiological boundary conditions. We look forward to the integration of these models into simulators of liver access surgery or radiotherapy planning systems.

# Appendix

<b>Dataset Name</b>	<b>Dataset size / MB</b>	<b>File Format Used</b>	<b>Number of breathing phases available</b>	<b>Details of breathing phases available</b>
<b>CLB</b>	705	hdr, img	10	Inhalation: 0, 10, 20, 30, 40, 50, 60, 70, 80, 90%
<b>Siemens</b>	717	DICOM	10	Inhalation: 20, 40, 60, 80, 100%  Exhalation: 0, 20, 40, 60, 80%
<b>MRI</b>	91.4	DICOM	3	Reference Intermediate Final

**Table 1**

**A summary of the acquired imaging datasets obtained after patient scanning.**

The CLB and Siemens datasets were substantially larger than the MRI dataset; they also offered a greater range of breathing phases for segmentation.

Absolute Values / mm	CLB dataset	Siemens dataset	MRI Phases 1-2	MRI Phases 1-3
Minimum	<b>0</b>	<b>0</b>	<b>0</b>	<b>0</b>
Maximum	<b>9.205</b>	<b>19.288</b>	<b>35.9342</b>	<b>87.6762</b>
Mean	<b>1.16287</b>	<b>1.53204</b>	<b>12.2614</b>	<b>31.4577</b>
RMS	<b>1.55828</b>	<b>2.84356</b>	<b>15.1989</b>	<b>40.578</b>

**Table 2**

A table showing the absolute values of distance error measurements when registered 3D surface models are compared to the original, segmented 3D surface model within the CLB, Siemens and MRI datasets (RMS, Root Mean Square).

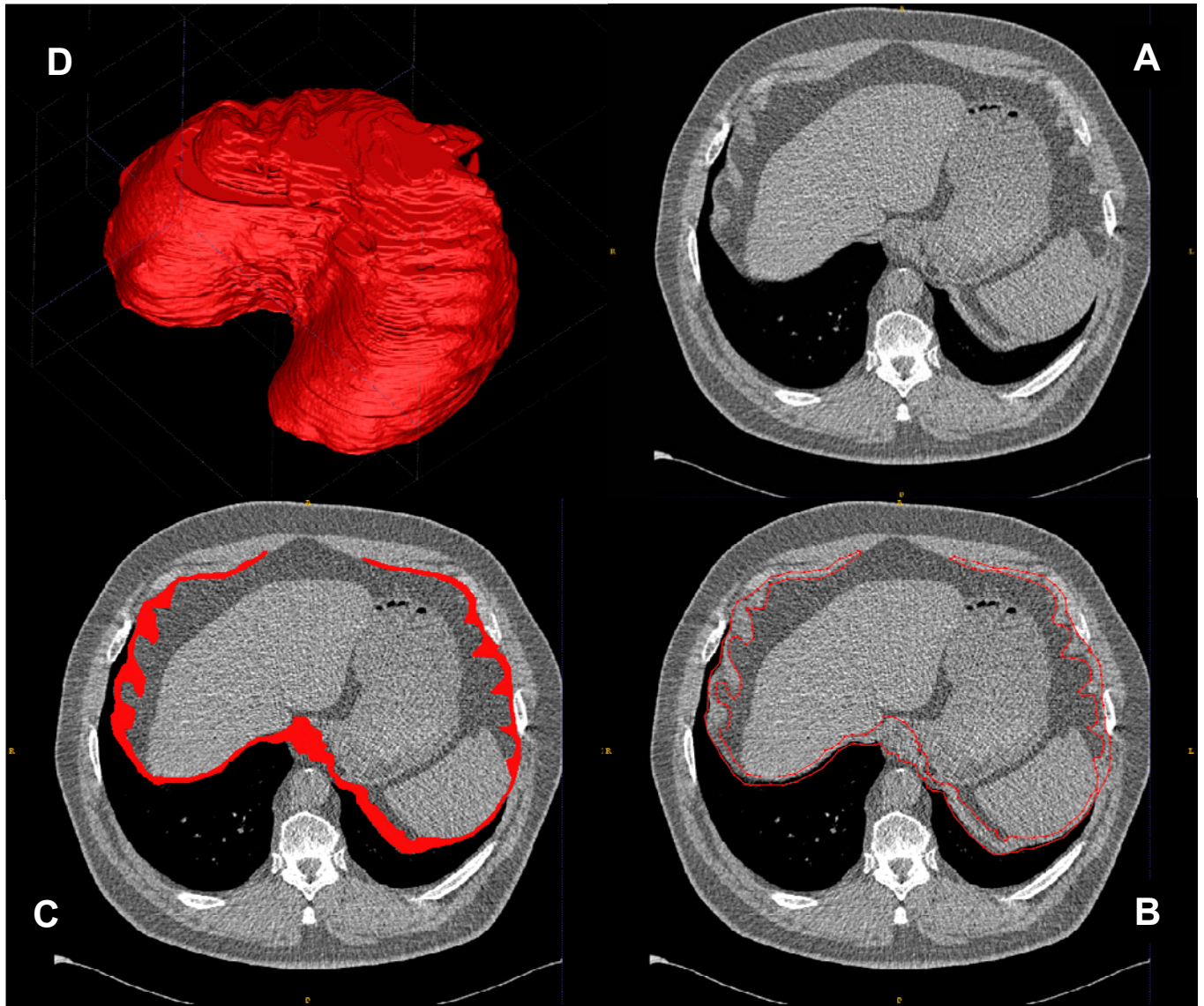


**Figure 1**

### **The Process of Manual Segmentation of the Diaphragm**

[A] Starting inferiorly, visual inspection is necessary to establish the boundaries of the diaphragm. [B] The polygon tool is used to form a closed contour around the diaphragm. [C] A colour label is assigned to the outlined structure, making the segmented diaphragm clearly visible on the slice. [D] Labels from many consecutive slices are exported as a 3D surface mesh as seen here.

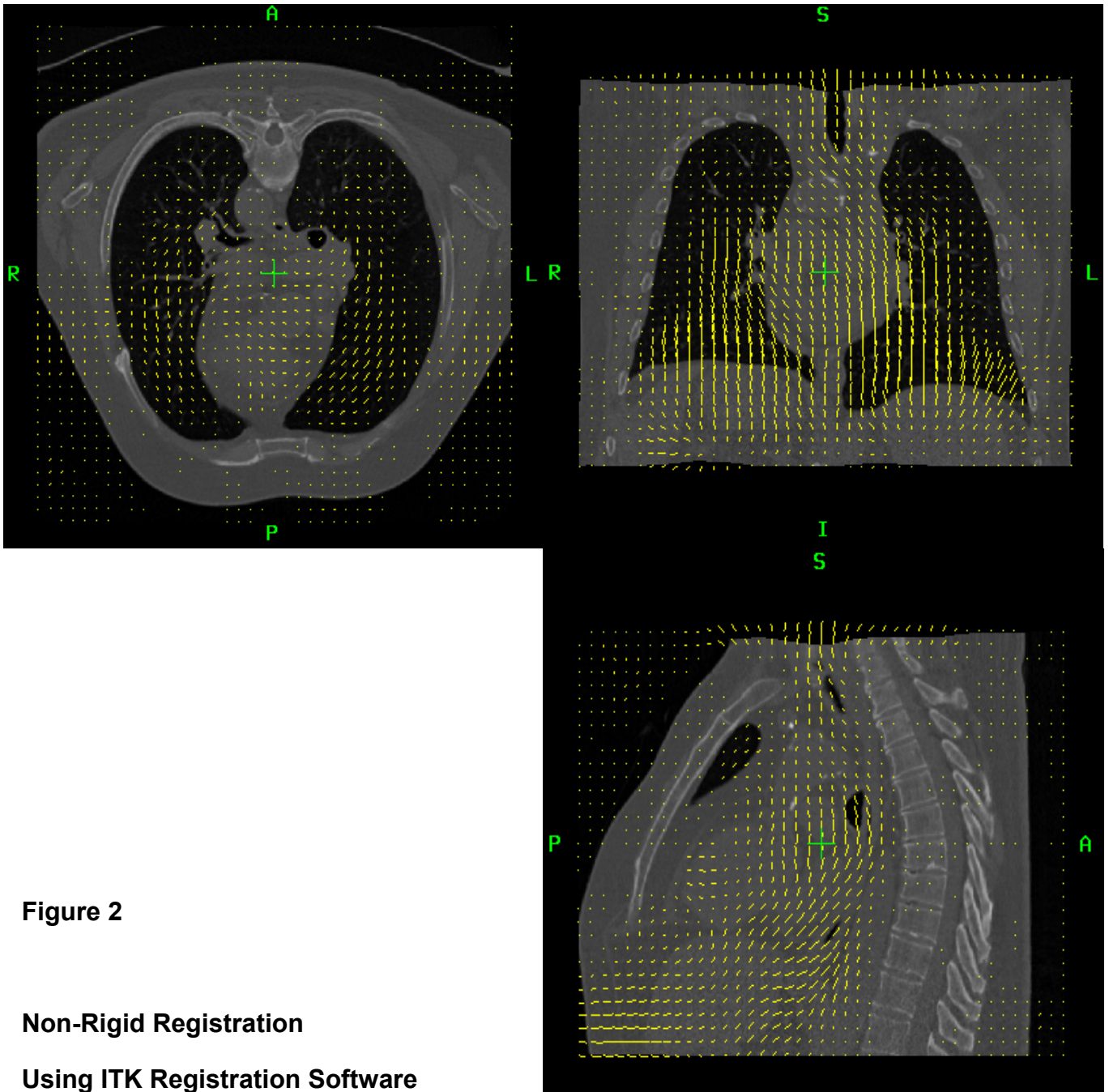


**Figure 2**  
**Non-Rigid Registration**  
**Using ITK Registration Software**

A transformation is generated from non-rigid registration, which estimates the positions of landmarks in a target image file, based on those in a source image file. Here, the yellow lines are vectors that represent displacements between the source and target image files.

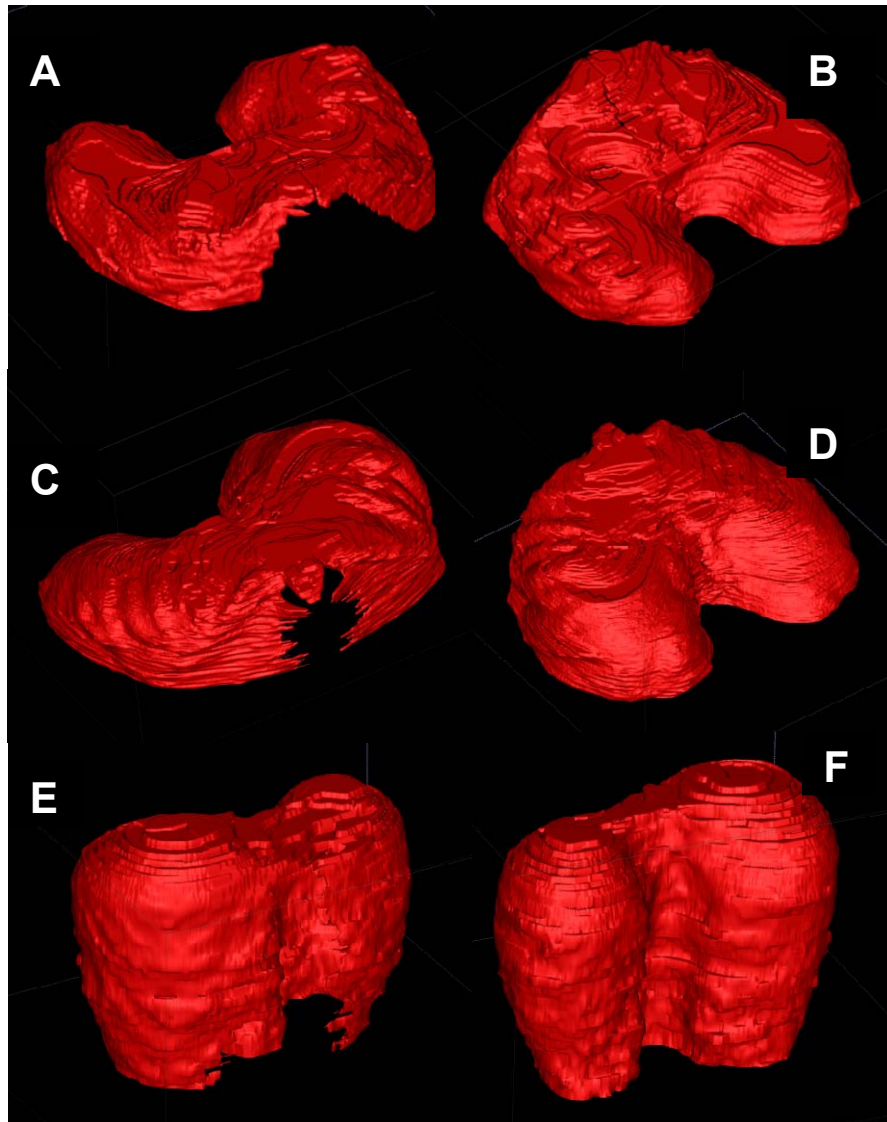


**Figure 3**

**Results of Diaphragm Segmentation**

CLB dataset, 90% inhalation, front [A] and back [B]

Siemens dataset, 100% inhalation, front [C] and back [D]

MRI dataset, phase 3, front [E] and back [F]

Hausdorff Values ↓

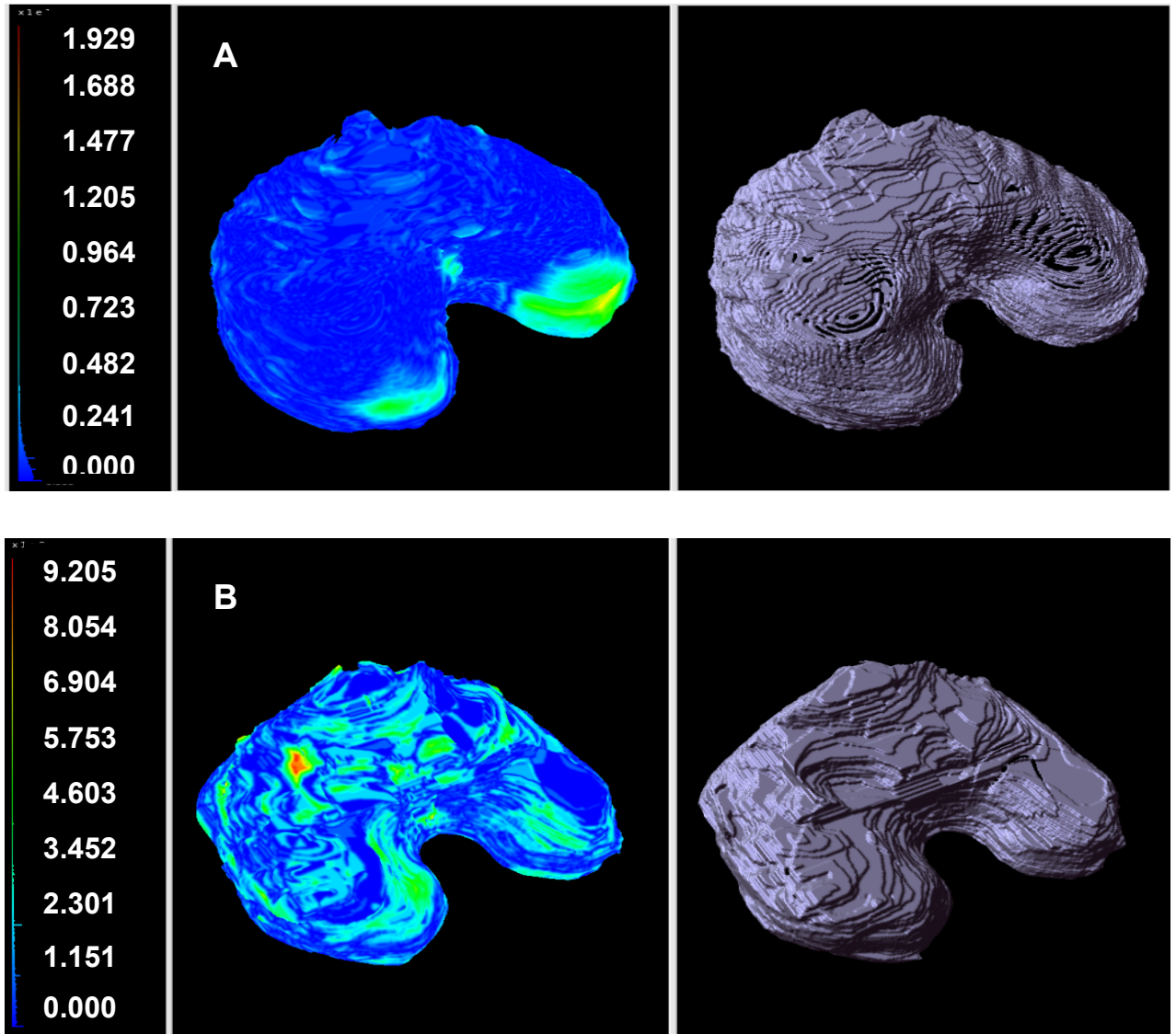


**Figure 4** Hausdorff distances, a measure of distance error, are displayed on a coloured scale in MESH software. The image on the left represents the Hausdorff distance between the surface of the diaphragm extracted from CT at the beginning and end of real inhalation. The image on the right represents the Hausdorff distance between the simulated end of inhalation and the real end of inhalation. **[A] Siemens dataset; [B] CLB dataset**

Hausdorff Values ↓

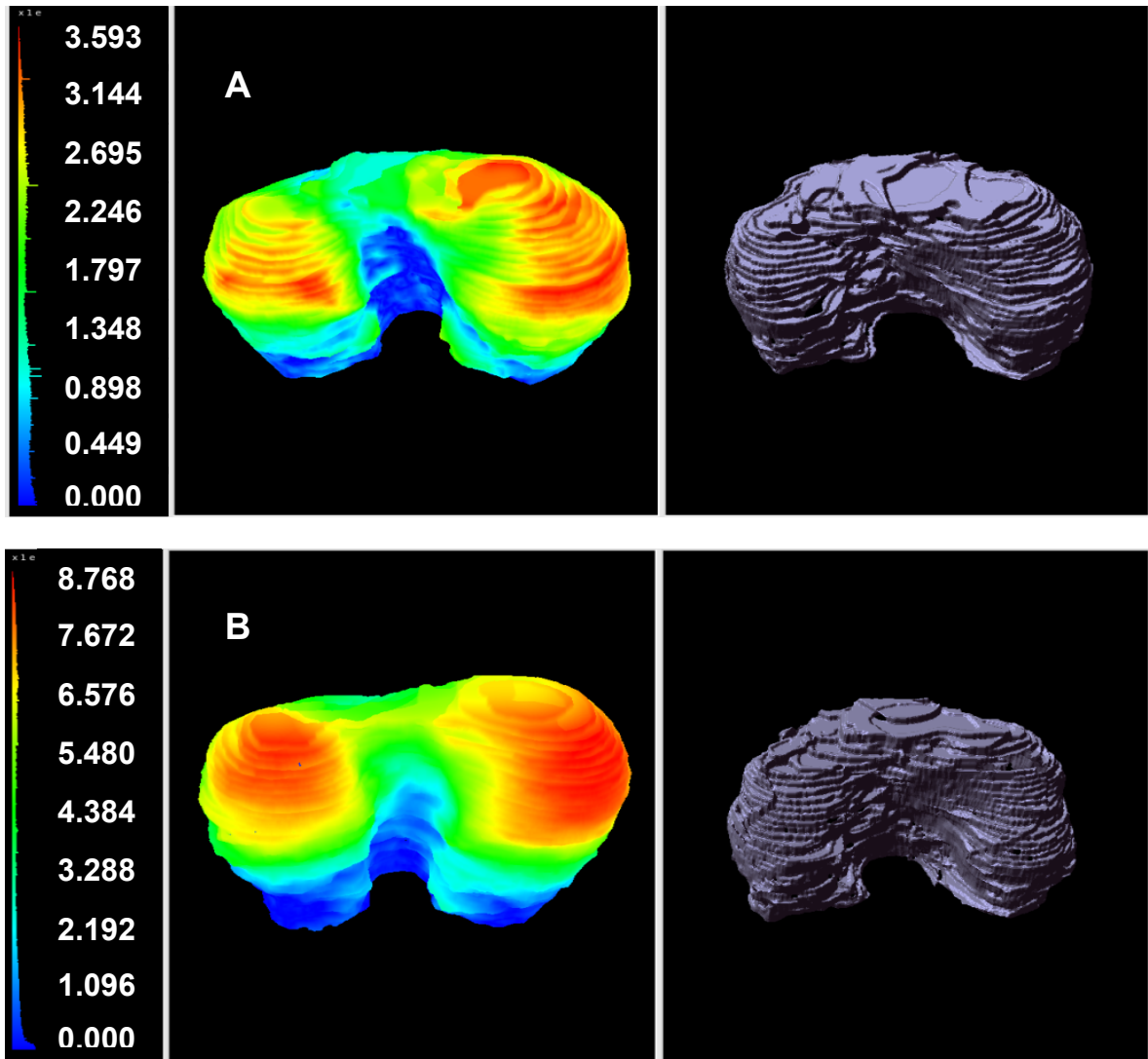


**Figure 5**

**Hausdorff distances calculated for the MRI dataset**

[A] The image on the left represents the Hausdorff distance between the surface of the diaphragm extracted from MRI dataset at the beginning and end of real inhalation.

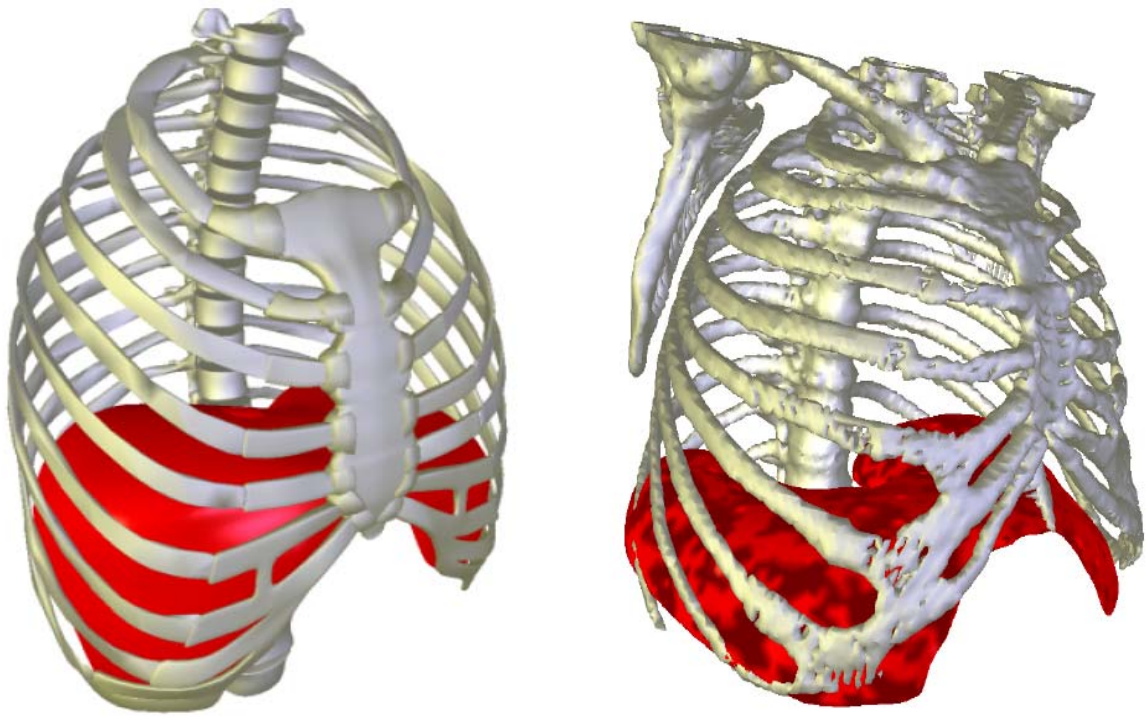


**Figure 6**

### **Final Diaphragm Model**

A commercial virtual anatomy model (Anatomium 3D by CF Lietzau 3D Special Service, left) is shown against our diaphragm model (right), consisting of a real, manually segmented diaphragm sourced from patient CT data, and an automatically segmented thoracic cage. Physiologically accurate diaphragm activity is modelled with synchronised rib expansion and contraction to simulate breathing.

## **Acknowledgements**

I would like to thank the following for their continued assistance in this study:

**Dr. Fernando Bello**, Senior Lecturer in Surgical Graphics and Computing

Division of Surgery, Oncology, Reproductive Biology and Anaesthetics  
St. Mary's Hospital  
London

**Dr. Pierre-Frédéric Villard**, Research Associate in Surgical Graphics and Computing

Division of Surgery, Oncology, Reproductive Biology and Anaesthetics  
St. Mary's Hospital  
London

**Dr. Vincent Luboz**, Research Associate in Surgical Graphics and Computing

Division of Surgery, Oncology, Reproductive Biology and Anaesthetics  
St. Mary's Hospital  
London

**Dr. Mohamad Hamady**, Consultant Interventional Radiologist

Radiology Department  
St. Mary's Hospital  
London

**Patients and staff of The Royal Liverpool University Hospital**

Prescot Street  
Liverpool,  
L7 8XP  
United Kingdom

**Patients and staff of Centre Léon-Bérard**

28, rue Laennec  
69373 Lyon  
Cedex 08  
France

## REFERENCES

- Adam A.** (2002) Interventional radiology in the treatment of hepatic metastases. *Cancer Treatment Reviews*, 28, 93-99.
- Aggarwal R, Moorthy K, Darzi A.** (2004) Laparoscopic skills training and assessment. *British Journal of Surgery*, 91, 1549-1558.
- Aggarwal R, Black SA, Hance JR, Darzi A, Cheshire NJW.** (2006) Virtual Reality Simulation Training can Improve Inexperienced Surgeon's Endovascular Skills. *European Journal of Vascular and Endovascular Surgery*, 31, 588-593.
- Aggarwal R, Ward J, Balasundaram I, Sains P, Athanasiou T, Darzi A.** (2007) Proving the Effectiveness of Virtual Reality Simulation for Training in Laparoscopic Surgery. *Annals of Surgery*, 246, 771-779.
- Al-Nahhas A.** (2007) Treatment of liver tumours with  $^{90}\text{Y}$ -Microspheres. *Presented as part of Imperial College London Surgery and Anaesthesia BSc course.* Hammersmith Hospital, London.
- Baegert C, Villard C, Schreck P, Soler L, Gangi A.** (2007) Trajectory optimization for the planning of percutaneous radiofrequency ablation of hepatic tumours. *Computer Aided Surgery*, 12 (2), 82-90.
- Balter JM, Dawson LA, Kazanjian S, McGinn C, Brock KK, Lawrence T, Ten Haken R.** (2001) Determination of ventilatory liver movement via radiographic evaluation of diaphragm position. *International Journal of Radiation Oncology Biology Physics*, 51 (1), 267-270.
- Basdogan C, Sedef M, Harders M, Wesarg S.** (2007) VR-based simulators for training in minimally invasive surgery. *IEEE Computer Graphics and Applications*, 27 (2), 54-66.
- Behr M, Thollon L, Arnoux P-J, Serre T, Berdah SV, Baque P, Brunet C.** (2006) 3D reconstruction of the diaphragm for virtual traumatology. *Surgical and Radiologic Anatomy*, 28, 235-240.
- Bridges M, Diamond DL.** (1999) The financial impact of teaching surgical residents in the operating room. *American Journal of Surgery*, 177, 28-32.
- Clark TWI.** (2007) Chemical Ablation of Liver Cancer. *Techniques in Vascular and Interventional Radiology*, 10, 58-63.

- Clifford MA, Banovac F, Levy E, Cleary K.** (2002) Assessment of Hepatic Motion Secondary to Respiration for Computer Assisted Interventions. *Computer Aided Surgery*, 7, 291-299.
- Cosman PH, Cregan PC, Martin CJ, Cartmill JA.** (2002) Virtual Reality Simulators: Current Status in Acquisition and Assessment of Surgical Skills. *ANZ Journal of Surgery*, 72, 30-34.
- Craighero S, Promayon E, Baconnier P, Lebas JF, Coulomb M.** (2005) Dynamic echo-planar MR imaging of the diaphragm for 3D dynamic analysis. *European Journal of Radiology*, 15, 742-748.
- Crum WR, Hartkens T, Hill DLG.** (2004) Non-rigid image registration: theory and practice. *The British Journal of Radiology*, 77, S140-S153.
- Cuschieri A, Francis N, Crosby J, Hanna GB.** (2001) What do master surgeons think of surgical competence and revalidation? *The American Journal of Surgery*, 182, 110-116.
- Darzi A, Mackay S.** (2002) Recent advances in minimal access surgery. *British Medical Journal*, 324, 31-34.
- Davies SC, Hill AL, Holmes RB, Halliwell M, Jackson PC.** (1994) Ultrasound quantification of respiratory organ motion in the upper abdomen. *The British Journal of Radiology*, 67 (803), 1096-1102.
- Dawson SL, Kaufman JA.** (1998). The imperative for medical simulation. *Proceedings of the IEEE*, 8 (3), 479-483.
- Dawson LA, Brock KK, Kazanjian A, Fitch D, McGinn C, Lawrence TS, Ten Haken RK, Balter J.** (2001) The Reproducibility of Organ Position Using Active Breathing Control (ABC) During Liver Radiotherapy. *International Journal of Radiation Oncology Biology Physics*, 51 (5), 1410-1421.
- Dent TL, Ponsky JL, Berci G.** (1991) Minimal access general surgery: the dawn of a new era. *The American Journal of Surgery*, 161, 323.
- Dhawan AP, Arata L.** (1993) Segmentation of medical images through competitive learning. *Computer Methods and Programs in Biomedicine*, 40, 203-215.
- Dick EA, Taylor-Robinson SD, Thomas HC, Gedroyc WMW.** (2002) Ablative therapy for liver tumours. *Gut*, 50, 733-739.
- Didier A-L, Villard P-F, Bayle J-Y, Beuve M, Shariat B.** (2007) Breathing Thorax Simulation based on Pleura Physiology and Rib Kinematics. *Proceedings of*

*the International Conference on Medical Information Visualisation - BioMedical Visualisation, 35-42.*

**Drake RL, Vogl W, Mitchell AWM.** (2005) *Gray's Anatomy for Students*. London, Churchill Livingstone.

**Dunkin B, Adrales GL, Apelgren K, Mellinger JD.** (2007) Surgical simulation: a current review. *Surgical Endoscopy*, 21, 357-366.

**Fried MP, Satava R, Weghorst S, Gallagher AG, Sasaki C, Ross D, Sinanan M, Uribe JI, Zeltsan M, Arora H, Cuellar H.** (2004) Identifying and reducing errors with surgical simulation. *Quality and Safety in Health Care*, 13 (Suppl. 1), 19-26.

**Gale ME.** (1986) Anterior Diaphragm: Variations in CT Appearance. *Radiology*, 161 (3), 635-639.

**Gillams AR.** (2005) Image guided tumour ablation. *Cancer Imaging*, 5, 103-109.

**Giraud P, Yorke E, Jiang S, Rosenzweig K, Magera G.** (2006) Reduction of organ motion effects in IMRT and conformal 3D radiation delivery by using gating and tracking techniques. *Cancer Radiothérapie*, 10 (5), 269-282.

**Hanna GB, Cresswell AB, Cuschieri A.** (2002) Shadow depth cues and endoscopic task performance. *Archives of Surgery*, 137 (10), 1166-1169.

**Hart R, Karthigasu K.** (2007) The benefits of virtual reality simulator training for laparoscopic surgery. *Current Opinion in Obstetrics and Gynaecology*, 19, 297-302.

**Hawkins MA, Dawson LA.** (2006) Radiation Therapy for Hepatocellular Carcinoma: From Palliation to Cure. *Cancer*, 106 (8), 1653-1663.

**Higgins H, Berger DL.** (2006) RFA for Liver Tumors: Does It Really Work? *The Oncologist*, 11, 801-808.

**Hinshaw JL, Lee FT.** (2007) Cryoablation for Liver Cancer. *Techniques in Vascular and Interventional Radiology*, 10, 47-57.

**Huttenlocher DP, Klanderman GA, Rocklidge WJ.** (1993) Comparing Images Using the Hausdorff Distance. *IEEE Transactions on Pattern Analysis and Machine Intelligence*, 15 (9), 850-863.

**Institute of Medicine of the National Academy of Sciences.** (2000) *To Err is Human*.  
[Online] Available from:

<http://books.nap.edu/openbook.php?isbn=0309068371> [Accessed 10 May 2008].

- Jaffray B.** (2005) Minimally invasive surgery. *Archives of Disease in Childhood*, 90, 537-542.
- Kang Y, Engelke K, Kalender WA.** (2004) Interactive 3D editing tools for image segmentation. *Medical Image Analysis*, 8, 35-46.
- Kirilova A, Lockwood G, Math M, Choi P, Bana N, Haider MA, Brock KK, Eccles C, Dawson LA.** (2008) Three-Dimensional Motion of Liver Tumors Using Cine-Magnetic Resonance Imaging. *International Journal of Radiation Oncology Biology Physics* [Ahead of print].
- Krishnan S, Dawson LA, Seong J, Akine Y, Beddar S, Briere TM, Crane C, Mornex F.** (2008) Radiotherapy for hepatocellular carcinoma: an overview. *Annals of Surgical Oncology*, 15 (4), 1015-1024.
- Lee AC, Haddad MJ, Hanna GB.** (2007a) Influence of instrument size on endoscopic task performance in paediatric intracorporeal knot tying: smaller instruments are better in infants. *Surgical Endoscopy*, 21 (11), 2086-2090.
- Lee AC.** (2007b) Are you working comfortably and safely? Presented as part of Imperial College London Surgery and Anaesthesia BSc course. St. Mary's Hospital, London.
- Lencioni R, Cioni D, Crocetti L, Bartolozzi C.** (2004) Percutaneous Ablation of Hepatocellular Carcinoma: State-of-the-Art. *Liver Transplantation*, 10 (2, Suppl. 1), 91-97.
- Lencioni R, Della Pina C, Bartolozzi C.** (2005) Percutaneous image-guided radiofrequency ablation in the therapeutic management of hepatocellular carcinoma. *Abdominal Imaging*, 30, 401-408.
- Llovet JM, Beaugrand M.** (2003) Hepatocellular carcinoma: present status and future prospects. *Journal of Hepatology*, 38 (Suppl. 1), 36-49.
- Maintz JB, Viergever MA.** (1998) A survey of medical image registration. *Medical Image Analysis*, 2 (1), 1-36.
- Marescaux J, Clément J-M, Tasseti V, Koehl C, Cotin S, Russier Y, Mutter D, Delingette H, Ayache N.** (1998) Virtual Reality Applied to Hepatic Surgery Simulation: The Next Revolution. *Annals of Surgery*, 228 (5), 627-634.

- Mishra RK, Hanna GB, Brown SI, Cuschieri A.** (2004) Optimum shadow-casting illumination for endoscopic task performance. *Archives of Surgery*, 139 (8), 889-892.
- Moorthy K, Munz Y, Sarker SK, Darzi A.** (2003) Objective assessment of technical skills in surgery. *British Medical Journal*, 327, 1032-1037.
- Morton JH.** (2000) Qualities of a Successful Surgeon. *Archives of Surgery*, 135, 1477.
- Müller SA, Maier-Hein L, Mehrabi A, Pianka F, Rietdorf U, Wolf I, Grenacher L, Richter G, Gutt CN, Schmidt J, Meinzer HP, Schmied BM.** Creation and establishment of a respiratory liver motion simulator for liver interventions. *Medical Physics*, 34 (12): 4605-4608.
- Mutaf YD, Brinkmann DH.** (2008) Optimization of Internal Margin to Account For Dosimetric Effects of Respiratory Motion. *International Journal of Radiation Oncology Biology Physics*, 20 (5), 1561-1570.
- Panicek DM, Benson CB, Gottlieb RH, Heitzman ER.** (1988) The diaphragm: Anatomic, pathologic and radiologic considerations. *Radiographics*, 8 (3), 385-425.
- Pickersgill T.** (2001) The European working time directive for doctors in training. *British Medical Journal*, 323, 1266.
- Qatarneh SM, Noz ME, Hyödynmaa S, Maguire GQ, Kramer EL, Crafoord J.** (2003) Evaluation of a segmentation procedure to delineate organs for use in construction of a radiation therapy planning atlas. *International Journal of Medical Informatics*, 69, 39-55.
- Rangayyan RM, Vu RH, Boag GS.** (2008) Automatic Delineation of the Diaphragm in Computed Tomographic Images. *Journal of Digital Imaging* [Ahead of print].
- Reitinger B, Bornik A, Beichel R, Schmalsteig D.** (2006) Liver surgery planning using virtual reality. *IEEE Computer Graphics and Applications*, 26 (6), 36-47.
- Reznick RK.** (1993) Teaching and testing technical skills. *American Journal of Surgery*, 165, 358-361.
- Rietzel E, Chen GTY, Choi NC, Willet CG.** (2005) Four-Dimensional Image-Based Treatment Planning: Target Volume Segmentation and Dose Calculation in the Presence of Respiratory Motion. *International Journal of Radiation Oncology Biology Physics*, 61 (5), 1535-1550.

- Rohlfing T, Maurer CR, O'Dell WG, Zhong J.** (2004) Modeling liver motion and deformation during the respiratory cycle using intensity-based nonrigid registration of gated MR images. *Medical Physics*, 31 (3), 427-432.
- Roberts KE, Bell RL, Duffy AJ.** (2006) Evolution of surgical skills training. *World Journal of Gastroenterology*, 12 (20), 3219-3224.
- Sarker SK, Patel B.** (2007) Simulation and surgical training. *International Journal of Clinical Practice*, 61 (12), 2120-2125.
- Sarrut D, Boldea V, Ayadi M, Badel J-N, Ginestet C, Clippe S, Carrie C.** (2005) Nonrigid Registration Method To Assess Reproducibility of Breath-Holding With ABC in Lung Cancer. *International Journal of Radiation Oncology Biology Physics*, 61 (2), 594-607.
- Satava RM.** (1993) Virtual reality surgical simulator: the first steps. *Surgical Endoscopy*, 7, 203-205.
- Satava RM.** (2001a) Surgical Education and Surgical Simulation. *World Journal of Surgery*, 25, 1484-1489.
- Satava RM.** (2001b) Accomplishments and challenges of surgical simulation: dawning of the next-generation surgical education. *Surgical Endoscopy*, 15, 232-241.
- Seymour NE, Røtnes JS.** (2006) Challenges to the development of complex virtual reality surgical simulations. *Surgical Endoscopy*, 20, 1774-1777.
- Sharma KC, Kabinoff GK, Ducheine Y, Tierney J, Brandstetter RD.** (1997) Laparoscopic surgery and its potential for medical complications. *Heart and Lung: The Journal of Acute and Critical Care*, 26 (1), 52-64.
- Sinnatamby CS** (ed.) (1999) *Last's Anatomy: Regional and Applied*. 10<sup>th</sup> edition. London, Churchill Livingstone.
- Smith M, Faraci A, Bello F.** (2004) Segmentation and generation of patient-specific 3D models of anatomy for surgical simulation. *Studies in Health Technology and Informatics*, 98, 360-2.
- Suramo I, Päivänsalo M, Myllylä V.** (1984) Cranio-caudal movements of the liver, pancreas and kidneys in respiration. *Acta Radiologica: Diagnosis*, 25 (2), 129-131.
- The Internet Classics Archive.** (1994) *Aphorisms, by Hippocrates*. [Online] Available from: <http://classics.mit.edu/Hippocrates/aphorisms.html> [Accessed 10 May 2008].

- Tse RV, Guha C, Dawson LA.** (2008) Conformational radiotherapy for hepatocellular carcinoma. *Critical Reviews in Oncology/Haematology*. [Ahead of print].
- Vedam SS, Kini VR, Keall PJ, Ramakrishnan V, Mostafavi H, Mohan R.** (2003) Quantifying the predictability of diaphragm motion during respiration with a noninvasive external marker. *Medical Physics*, 30 (4), 505-513.
- Vidal FP, Bello F, Brodlie KW, John NW, Gould D, Phillips R, Avis NJ.** (2006) Principles and Applications of Computer Graphics in Medicine. *Computer Graphics*, 25 (1), 113-137.
- Villard C, Soler L, Gangi A.** (2005) Radiofrequency ablation of hepatic tumours: simulation, planning and contribution of virtual reality and haptics. *Computer Methods in Biomechanics and Biomedical Engineering*, 8 (4), 215-227.
- Villard P-F, Bourne W, Acharya M, Bello F.** (2008) Real Time Physically-Based Simulation of Diaphragm Motion for Lung Cancer Radiotherapy and Liver Access Procedures. [Unpublished].
- Visser BC, Parks RW, Garden OJ.** (2008) Open cholecystectomy in the laparoscopic era. *The American Journal of Surgery*, 195, 108-114.
- Weir J, Abrahams PH.** (2003) *Imaging Atlas of Human Anatomy*. 3<sup>rd</sup> edition. London, Mosby.
- Westebring-Van Der Putten EP, Goossens RHM, Jakimowicz JJ, Dankelman J.** (2008) Haptics in minimally invasive surgery – a review. *Minimally Invasive Therapy*, 17 (1), 3-16.
- Yushkevich PA, Piven J, Hazlett HC, Smith RG, Ho S, Gee JC, Gerig G.** (2006) User-guided 3D active contour segmentation of anatomical structures: Significantly improved efficiency and reliability. *NeuroImage*, 31, 1116-1128.
- Zitová B, Flusser J.** (2003) Image registration methods: a survey. *Image and Vision Computing*, 21, 977-1000.